ACS Macro Letters

pubs.acs.org/macroletters Letter

Polymer Dynamics in Block Copolymer Electrolytes Detected by Neutron Spin Echo

Whitney S. Loo, Antonio Faraone, Lorena S. Grundy, Kevin W. Gao, and Nitash P. Balsara*

Cite This: ACS Macro Lett. 2020, 9, 639−645 Read Online

ACCESS | Metrics & More | Article Recommendations | Supporting Information

ABSTRACT: Polymer chain dynamics of a nanostructured block copolymer electrolyte, polystyrene-*block*-poly(ethylene oxide) (SEO) mixed with lithium bis(trifluoromethanesulfonyl)imide (LiTFSI) salt, are investigated by neutron spin echo (NSE) spectroscopy on the 0.1−100 ns time scale and analyzed using the Rouse model at short times ($t \leq 10$ ns) and the reptation tube model at long times ($t \geq 50$ ns). In the Rouse regime, the monomeric friction coefficient increases with increasing salt concentration, as seen previously in homopolymer electrolytes. In the reptation regime, the tube diameters, which represent entanglement constraints, decrease with increasing salt concentration. The normalized longest molecular relaxation time, calculated from the NSE results, increases with increasing salt concentration. We argue that quantifying chain motion in the presence of ions is essential for predicting the behavior of polymer-electrolyte-based batteries operating at large currents.

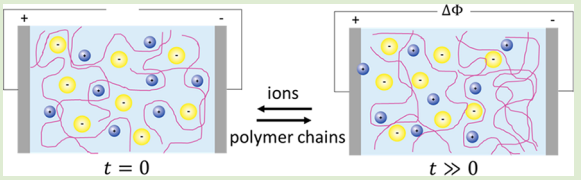

It is becoming increasingly clear that the next generation of rechargeable batteries for the emerging clean energy landscape will require electrolytes that are fundamentally different from those used in today's lithium-ion batteries. Current electrolytes in lithium-ion batteries are comprised of mixtures of cyclic and linear carbonates and a lithium salt. Polymer electrolytes, which are mixtures of polymers and a lithium salt, have the potential to improve battery safety as they are less flammable than the organic solvents used currently.[1] Efforts to characterize polymer electrolytes have focused on quiescent systems or systems under very small applied potentials (e.g., 10 mV).[2,3] Under these conditions, it is reasonable to focus on the motion of ions; the motion of polymer chains on larger length scales can be safely neglected. However, in electrolytic applications, such as batteries in electric vehicles, ion transport occurs under large applied dc potentials (e.g., 4 V). Under these conditions, significant salt concentration gradients develop due to the well-established competition between diffusion and migration.[4] Since the salt concentration in the electrolyte must be uniform before the polymer-electrolyte-based battery is turned on, the polymer chains must diffuse away from regions of high salt concentration toward regions of low salt concentration during battery operation. The purpose of this Letter is to elucidate the molecular underpinnings of this process. We present the first study of polymer electrolytes using neutron spin echo (NSE) spectroscopy.

A popular approach for characterizing ion transport in electrolytes is ac impedance spectroscopy, which reflects the oscillation of ions in response to a small ac potential.[2,5,6] Another popular approach is pulse-field gradient NMR, wherein the Brownian motion of ions is quantified in the absence of an applied potential.[3,7−10] In these cases, the translation of ions can be accommodated by segmental relaxation of the polymer chains.[11−21] Thus, ionic conductivity of a well-studied polymer electrolyte, a mixture of poly(ethylene oxide) (PEO) and lithium bis(trifluoromethanesulfonyl)imide (LiTFSI) salt measured by ac impedance spectroscopy, can be explained entirely by the segmental relaxation quantified by quasi-elastic neutron scattering (QENS).[15] To our knowledge, no attempt has been made to study the relaxation processes that govern polymer electrolytes under large applied potentials.

One advantage of polymer electrolytes over liquid electrolytes is their ability to exert stress on the electrodes. This is believed to be the key to enabling rechargeable batteries with lithium metal anodes,[22] which is a promising approach to significantly increase the energy density of rechargeable batteries.[23,24] Linear polymers are viscoelastic liquids and thus are unable to withstand stress in the long time limit. Cross-linking can increase their mechanical properties but slows down segmental relaxation, which in turn slows down ion transport.[25] A better approach for creating solid polymer electrolytes is through the self-assembly of block copolymers, which can microphase separate into ionically conductive and mechanically rigid domains.[26−29]

In this Letter, we quantify segmental motion and polymer dynamics in a series of block copolymer electrolytes using

Received: March 26, 2020
Accepted: April 10, 2020

https://dx.doi.org/10.1021/acsmacrolett.0c00236
ACS Macro Lett. 2020, 9, 639−645

NSE. The time-scales covered by our experiments range from 0.1 to 100 ns, which correspond to polymer dynamics on the Angstrom to nanometer length scales. At short times (0.1−10 ns), polymer chains obey Rouse dynamics, and their segmental motion is quantified by an effective friction coefficient, ζ, of the monomer units.[30,31] At longer times (10−100 ns), the motion of polymer segments of a "test-chain" is constrained by the presence of neighboring chains. In the theory of Doi, Edwards, and de Gennes, these constraints are represented by a tube with diameter, d, that runs down the primitive path of the "test-chain".[31,32] We are not aware of any prior studies on either polymer electrolytes or block copolymers (with or without salt) that cover both regimes. Previous studies on these systems using NSE are limited to the Rouse regime ($t \leq$ 20 ns).[15,18,33] Previous studies on nanostructured block copolymer electrolytes are limited to studying the cooperative grain dynamics on the 10^{-2}−10^{2} s time scale.[34]

The block copolymer electrolyte of interest is a well-studied model system: polystyrene-*block*-poly(ethylene oxide) (SEO) mixed with LiTFSI (SEO/LiTFSI). Two SEO copolymers with similar compositions were synthesized by living anionic polymerization:[35−37] deuterated PS-*b*-deuterated PEO (ddSEO) ($M_{n,dPS}$ = 4.9 kg mol^{-1}, $M_{n,dPEO}$ = 23.6 kg mol^{-1}, ϕ_{EO} = 0.82, PDI = 1.05) and deuterated PS-*b*-hydrogenated PEO (dhSEO) ($M_{n,dPS}$ = 5.1 kg mol^{-1}, $M_{n,hPEO}$ = 14.4 kg mol^{-1}, ϕ_{EO} = 0.73, PDI = 1.05). Detailed information on the synthesis is provided in the Supporting Information. The PEO blocks of both copolymers are well above the entanglement molecular weight, M_e = 2 kg mol^{-1}. The preparation of the SEO/LiTFSI electrolytes is described elsewhere.[38] The samples used were blends of 20% dhSEO and 80% ddSEO by volume (the densities of dhSEO and ddSEO are 1.10 and 1.11 g cm^{-3}, respectively, at 90 °C). LiTFSI was added to the copolymer blends such that the final molar salt ratios, $r = \frac{[Li]}{[EO]}$, were 0, 0.025, 0.075, and 0.10. The block copolymer system was designed such that the NSE data are dominated by relaxation of the PEO segments as they interact with salt ions; in particular, the incoherent background from the PEO chains is minimized at the scattering vectors, Q, chosen for NSE.[39]

Small-angle neutron scattering (SANS) experiments were performed at 90 °C on the NGB-30m beamline at the NIST Center for Neutron Research (NCNR, Gaithersburg, MD). Sample preparation for the SANS experiments is described elsewhere.[40] Measurements were performed such that the Q range covered was from 0.003 to 0.4 Å^{-1}.[41] The total scattering intensity was corrected for detector sensitivity, background, and empty cell contributions, as well as sample transmission and thickness.[42,43] Single-chain PEO dynamics were obtained using the NGA Neutron Spin Echo Spectrometer (NSE) at the NIST Center for Neutron Research (NCNR, Gaithersburg, MD). Sample preparation was similar to that of the SANS samples. The measurements were performed at 363 and 393 K using wavelengths of λ = 11 Å for Fourier times up to 100 ns and a wave vector range of Q = 0.11 to 0.20 Å^{-1}. Additional measurements were performed at λ = 6 Å for Fourier times up to 20 ns for Q = 0.11 to 0.20 Å^{-1}. Overlapping NSE data taken at λ = 6 and 11 Å for 0.1 $\leq t$ (ns) $\leq$ 30 are shown in the Supporting Information. A standard carbon sample was used to determine the instrument resolution. Data were corrected for background using an empty holder using the software DAVE.[44]

The SANS profiles for SEO/LiTFSI mixtures after subtracting the incoherent background, $I_{coh}(Q)$, at 90 °C for r = 0, 0.025, 0.075, and 0.10, are shown in Figure 1. All profiles contain a primary peak at $Q = Q^*$ and a higher order peak at

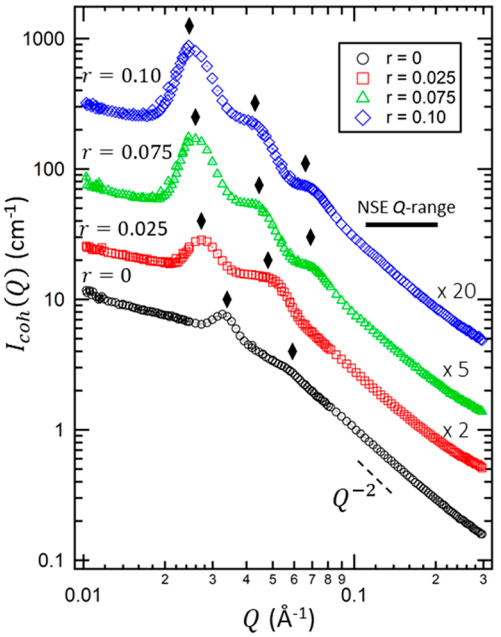

Figure 1. SANS profiles, $I_{coh}(Q)$, of SEO/LiTFSI mixtures at different salt concentrations, $0 \leq r \leq 0.10$, at 90 °C. Error bars represent one standard deviation and are smaller than the data points. Curves are offset vertically for clarity (scaling factors are given at the high-Q intercept). Diamonds represent the primary scattering peak, Q^*, and the higher order scattering peaks at $Q = \sqrt{3}\,Q^*$ and $\sqrt{7}\,Q^*$. The bar at high-Q represents the scattering vector range chosen for the NSE experiments, $0.11 \leq Q$ (Å^{-1}) ≤ 0.20. An example of the scaling for a Gaussian chain, Q^{-2}, is shown in the high-Q regime.

$Q = \sqrt{3}\,Q^*$. At $r \geq 0.075$, an additional higher order peak at $Q = \sqrt{7}\,Q^*$ is seen. The SANS data indicate that the SEO/LiTFSI mixtures order into hexagonally packed PS cylinders in a salt-containing PEO matrix at all salt concentrations as expected based on previous studies of the phase behavior of SEO/LiTFSI.[45] As salt concentration increases, the scattering intensities of the Bragg scattering peaks increase due to increased segregation between the PS and PEO/LiTFSI blocks with increasing salt concentration.[45−47] The domain spacing, given by $D = \frac{2\pi}{Q^*}$, increases from 18.5 to 25.5 nm as r increases from 0 to 0.10, as expected.[48,49] The SANS data show that the ddSEO/dhSEO/LiTFSI blends are macroscopically homogeneous at all salt concentrations; at high-Q, the scattering intensity scales with Q^{-2}, indicative of scattering from polymer chains obeying random walk statistics (see Supporting Information).[50] The bar at high-Q in Figure 1 shows the range of scattering vectors covered by the NSE experiments, which corresponds to intradomain length-scales ensuring that the NSE experiments selectively probe the PEO/LiTFSI matrix phase.

The dynamic scattering function measured by NSE, $\frac{S(Q,t)}{S(Q,0)}$, is shown as a function of salt concentration and temperature in Figure 2. At short times, $t \leq 10$ ns, the data are consistent with the Rouse model,[30] which has been shown by Richter and co-workers[51] to be approximated by

https://dx.doi.org/10.1021/acsmacrolett.0c00236
ACS Macro Lett. 2020, 9, 639−645

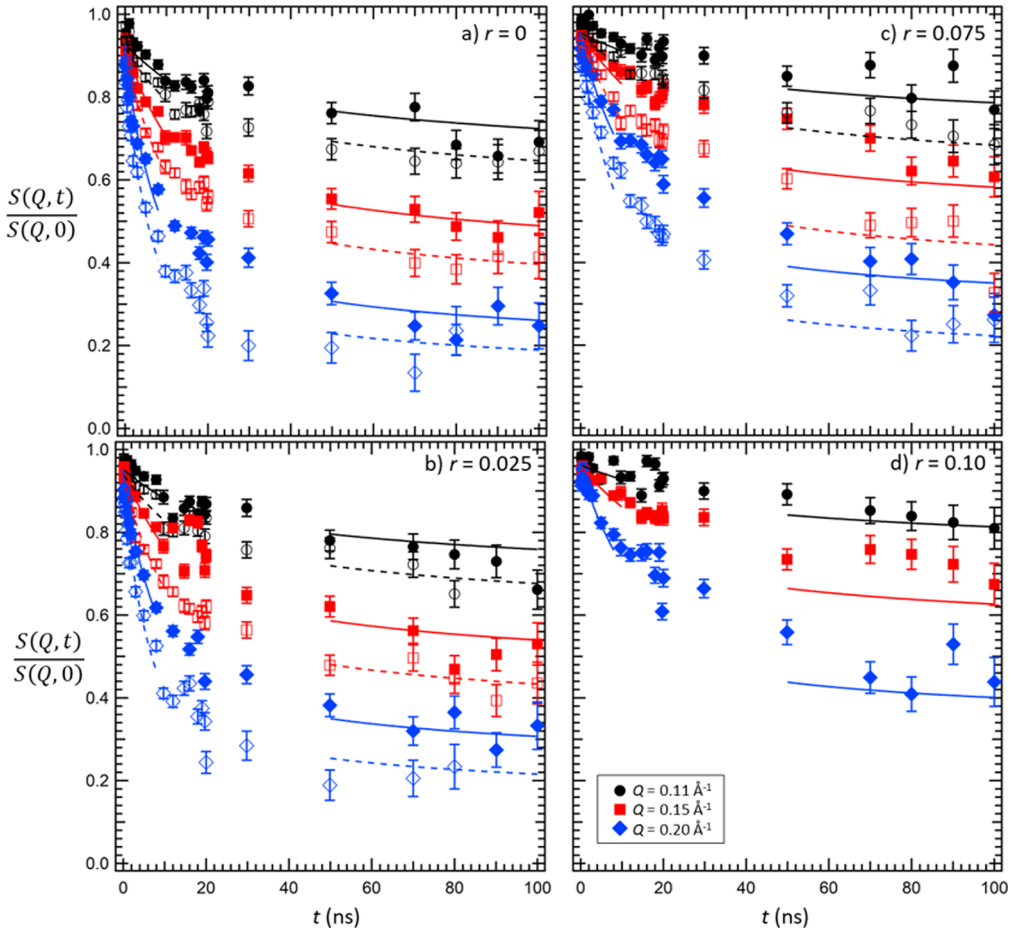

Figure 2. Dynamic scattering functions, $\frac{S(Q,t)}{S(Q,0)}$, determined from NSE for SEO/LiTFSI mixtures for Q = 0.11, 0.15, and 0.20 Å^{-1} at 90 °C (filled symbols) and 120 °C (open symbols) for different salt concentrations: (a) r = 0, (b) 0.025, (c) 0.075, and (d) 0.10. The error bars represent one standard deviation of the NSE data. At short times, $t \leq 10$ ns, the curves correspond to the Rouse model (eqs 1−3). At long times, $t \geq 50$ ns, the curves correspond to the tube model for reptation (eq 4). Solid lines represent fits to data taken at 90 °C and dashed lines represent fits to data taken at 120 °C.

$$\frac{S(Q,t)}{S(Q,0)} = \frac{12}{Q^2 l^2}\int_0^\infty du\ \exp\{-u - (\Omega_R t)^{1/2} h(u(\Omega_R t)^{-1/2})\} \quad (1)$$

with

$$h(y) = \frac{2}{\pi}\int_0^\infty dx\left(\frac{\cos xy}{x^2}\right)[1 - \exp(-x^2)] \quad (2)$$

and

$$(\Omega_R t)^{1/2} = \frac{Q^2 l^2}{6}\sqrt{Wt} \quad (3)$$

where the Rouse parameter is given by Wl^4 (l is the statistical segment length of the polymer and W is the elementary Rouse rate). The curves through the short time data in Figure 2 represent fits to eqs 1−3 for all Q values simultaneously with Wl^4 as the only adjustable parameter at both temperatures (see eq 3). A magnified view of the fits of eqs 1−3 through the low-t data is provided in the Supporting Information.

The data in Figure 2 show deviations from Rouse dynamics at $t \geq 20$ ns for all salt concentrations signaling the slowing down of segmental motion due to constraints imposed by the presence of other chains (see Supporting Information). The tube diameter, d, quantifies these constraints. The crossover from Rouse dynamics to local reptation occurs over the window from 20 to 50 ns. At long times, $t \geq 50$ ns, the data in Figure 2 were fit to the tube model proposed by de Gennes,[31,52] which gives

$$\frac{S(Q,t)}{S(Q,0)} = \left[1 - \exp\left(-\frac{Q^2 d^2}{36}\right)\right] S_{local}(Q,t) + \exp\left(-\frac{Q^2 d^2}{36}\right) S_{esc}(Q,t) \quad (4)$$

where $S_{local}(Q,t) = \exp\left(\frac{t}{\tau_0}\right)\mathrm{efrc}\left(\sqrt{\frac{t}{\tau_0}}\right)$ describes local reptation within the tube with characteristic time scale $\tau_0 = \frac{36}{Wl^4Q^4}$. $S_{esc}(Q,t)$ is related to the long-time dynamics of the confined chain and was neglected in this study ($S_{esc}(Q,t) = 1$). The Rouse parameter, Wl^4 was taken from the fits of eqs 1−3 in the low-t regime and used in eq 4 to determine the tube diameter, d. Equation 4 was fit simultaneously for all Q values at a given temperature leaving d as the only free parameter. The results and statistics for the fitting of eqs 1−4 are provided in the Supporting Information. We note that eqs 1−4 are derived for salt-free homopolymer systems and that no models currently exist for describing segmental dynamics and reptation of salt-containing polymer systems.

https://dx.doi.org/10.1021/acsmacrolett.0c00236
ACS Macro Lett. 2020, 9, 639−645

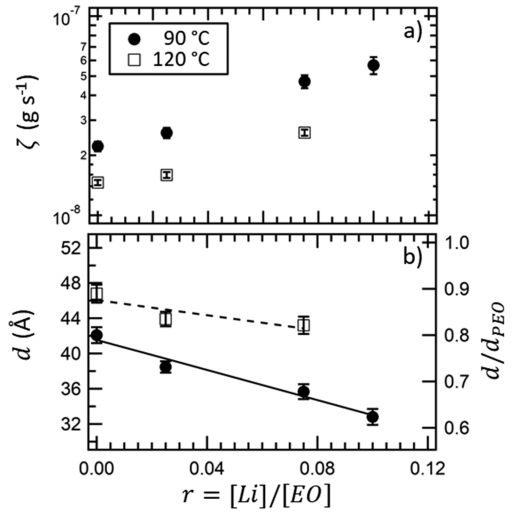

Figure 3. Results from fitting $\frac{S(Q,t)}{S(Q,0)}$ (Figure 2) in both the low and high t regions: (a) monomeric friction coefficient, ζ, (eq 5), (b) tube diameter (left axis), d, and normalized tube diameter (right axis), d/d_{PEO}, as a function of salt concentration, r, at 90 °C (filled symbols) and 120 °C (open symbols). Error bars represent one standard deviation from the fits. The lines in (b) are least-squares fits of the data through the equation, $\frac{d}{d_{PEO}} = ar + b$, where $a = -1.63 \pm 0.21$ and -0.82 ± 0.48, and $b = 0.80 \pm 0.01$ and 0.88 ± 0.02 for 90 and 120 °C, respectively, and the confidence intervals represent the standard deviations from the fits of $\frac{d}{d_{PEO}}$.

Figure 3 shows the results from the fits shown in Figure 2. The monomeric friction coefficient, ζ, is calculated from Wl^4 using eq 5,[51]

$$\zeta = \frac{3k_BT}{Wl^4}l^2 \tag{5}$$

where k_B is the Boltzmann constant and T is absolute temperature. The dependence of l on salt concentration for PEO/LiTFSI mixtures is reported in ref 40 at 90 °C. These values of l were used to calculate ζ according to eq 5, assuming that l is independent of temperature. The dependence of ζ on salt concentration is shown in Figure 3a at 90 °C (solid circles) and 120 °C (open squares). In the absence of salt ($r = 0$), ζ decreases with increasing temperature. These results are consistent with literature values for PEO homopolymer.[53] The monomeric friction coefficient increases with increasing salt concentration at a similar rate for both temperatures. At 90 °C, this rate matches that seen in PEO/LiTFSI systems.[15] The segmental dynamics on short-time scales, $t \leq 10$ ns, in a microphase separated block copolymer electrolyte is indistinguishable from that of the homopolymer electrolyte; see Supporting Information for details. In a related study, it has been shown that the presence of nanoparticles does not affect the segmental dynamics in polymer nanocomposites,[54] consistent with our finding that the PS-rich phase does not affect the segmental dynamics of the PEO-rich phase.

The dependence of tube diameter, d, on salt concentration is shown in Figure 3b. Our measured values of d increase with increasing temperature as typically seen in homopolymers due to a decrease in the number of entanglement constraints from increased chain mobility.[55] The tube diameter of PEO homopolymer, d_{PEO}, in the absence of salt at 125 °C is 52.6 Å.[53] The right y-axis in Figure 3b shows the ratio d/d_{PEO} as a function of salt concentration, where all data are normalized by d_{PEO} at 125 °C. In the neat state, d for SEO/LiTFSI at 120 °C is lower than that of PEO/LiTFSI at 125 °C. This deviation is more pronounced than what can be explained by temperature differences.[55−57] We attribute the decrease in tube diameter to the geometric constraints introduced by the PS microphase. It is thermodynamically unfavorable for portions of entangled chains near the interface of the two microphases to undergo reptation; in order to move around the entanglement constraints, portions of the PS block will need to enter the PEO/LiTFSI-rich phase.[58−60] This is consistent with previous findings that geometric confinement contracts tube diameters in polymer mixtures.[61] In addition, the tube diameter decreases with increasing salt concentration. As salt concentration increases, the coordination between Li^+ ions and the ether oxygens on the PEO backbone increases. Molecular dynamics simulations indicate that the Li^+ ions coordinate with either one or two PEO chains.[62] It is likely that coordination with two chains, which may be regarded as a temporary cross-link, has a more significant effect on chain entanglement. The decrease in d with r seen in Figure 3b is a reflection of this effect. The effect of salt concentration on the tube diameter is more pronounced at 90 °C relative to 120 °C by a factor of 2. This suggests that coordination effects are more significant at 90 °C, which is supported by MD simulations.[63,64] To our knowledge, these results provide the first measurements of the entanglement constraints, represented by tube diameters, as well as insight into polymer chain conformation in polymer electrolytes and block copolymers.

In a melt of entangled homopolymers with degree of polymerization N, the longest molecular relaxation time, τ_d, is given by[51]

$$\tau_d = \frac{\zeta N^3}{\pi^2 k_BT}\left(\frac{l^4}{d^2}\right) \tag{6}$$

which quantifies the time needed for a confined chain to escape the tube created by neighboring chains. This time-scale also determines the viscosity of the polymer melt.[65] Note that ζ, l and d are all functions of r. The fact that both parameters, ζ and d, obtained from the neat block copolymer are similar to that of PEO homopolymer indicates that eq 6 is a reasonable starting point to quantify the long-time dynamics of SEO/LiTFSI. In SEO electrolytes, there will be additional contributions to τ_d due to the presence of the PS microphase. Escape of SEO chains from their tubes will involve dragging PS segments through the PEO-rich microphase.[58−60] This factor is not accounted for in our estimate of τ_d. Due to this limitation, it is best to examine a normalized relaxation time, $\tau_{d,n}$, defined as

$$\tau_{d,n} = \frac{\tau_d(r)}{\tau_d(r=0)} \tag{7}$$

to quantify the effect of salt concentration on chain dynamics. At 90 °C, d^2 decreases by 39% over the range $0 \leq r \leq 0.10$, while ζ increases by a factor of 2.5 over the same window. Both factors slow down chain diffusion. However, the chain shrinks with added salt, l^4 decreases by 52% over the same window,[40] which will speed up chain diffusion. Therefore, the net effect of salt concentration on the polymer chain dynamics is that $\tau_{d,n}$ increases by a factor of 1.7 across our salt concentration window at 90 °C, as shown in Figure 4. The effect of salt concentration of chain diffusion is less pronounced at 120 °C.

https://dx.doi.org/10.1021/acsmacrolett.0c00236
ACS Macro Lett. 2020, 9, 639−645

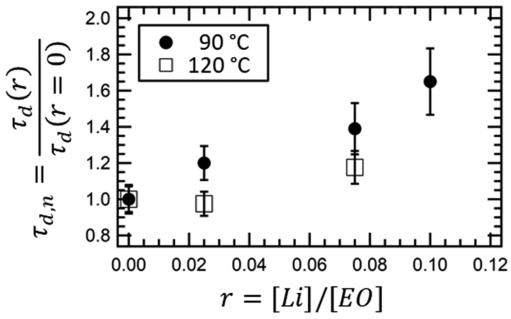

Figure 4. Normalized longest molecular relaxation time, $\tau_{d,n} = \tau_d(r)/\tau_d(r = 0)$, as a function of salt concentration, r, for SEO/LiTFSI at 90 °C (filled circles) and 120 °C (open squares) calculated from eqs 6 and 7. Error bars are propagations of the standard deviations of the fits of ζ and d from eqs 1−4.

It is important to note that these factors are lower bounds on the effect of added salt on the longest relaxation time of block copolymer electrolytes, as we have neglected contributions arising from the presence of the PS block.

Let us return to the discussion of a polymer-electrolyte-based battery operating at a large current. For completeness, we consider an SEO/LiTFSI electrolyte with $r = 0.05$ in a battery operating at 90 °C. The volume fraction of salt in this electrolyte is 0.16.[40] When a large enough current is applied, the volume fraction of the salt near the cathode will approach zero due to the well-established concept of concentration polarization.[4,66,67] Based on the data in ref 66, for a symmetric Li-SEO/LiTFSI-Li cell with a 250 μm thick electrolyte and a PEO volume fraction of 0.80, the current density at which the salt concentration in our SEO electrolyte would be zero at the cathode is 0.75 mA cm^{-2}, and the potential drop across the electrolyte would be 125 mV. In this case, the 16% of the electrolyte volume that was originally occupied by salt must be replaced by polymer due to the incompressibility constraint. Similarly, the salt concentration at the anode will increase to about $r = 0.10$, displacing polymer chains. The data in Figure 4 suggest that relaxation processes at the anode will be about 1.7 times slower than those at the cathode. While further work is necessary to substantiate this effect, the NSE results presented in Figures 3 and 4 provide the first insights into factors that may limit the performance of polymer-electrolyte-based batteries operating at high currents.

In conclusion, the effect of added salt on the polymer dynamics of a nanostructured block copolymer electrolyte are investigated using NSE on the 0.1−100 ns time scale and analyzed using the Rouse model at short times ($t \leq 10$ ns) and the reptation model at long times ($t \geq 50$ ns). The effect of salt concentration on the segmental dynamics in the Rouse regime matches the results of previous experiments on homopolymer electrolytes: monomeric friction increases with increasing salt concentration.[11−16] In the reptation regime, the tube diameter decreases with increasing salt concentration. We attribute this trend to temporary cross-links between neighboring chains arising from Li^+ ion coordination. The normalized longest molecular relaxation time, $\tau_{d,n}$, was calculated from the NSE results, and was found to increase with increasing salt concentration. All of the rich literature on polymer electrolytes is narrowly focused on the transport of ions under small applied fields or in the absence of applied fields.[7,17−21,29] We posit that our measurements of dynamics at long times (50−100 ns) are relevant to the operation of polymer-electrolyte-containing batteries at high currents, wherein the diffusion of salt ions in one direction must induce diffusion of polymer chains in the opposite direction.

■ ASSOCIATED CONTENT

Supporting Information

The Supporting Information is available free of charge at https://pubs.acs.org/doi/10.1021/acsmacrolett.0c00236.

Detailed information on polymer synthesis, quantitative analysis of the scattering experiments, results of fitting procedures shown in Figure 2, and reproduced data on PEO/LiTFSI for direct comparison from refs 15 and 40 (PDF)

■ AUTHOR INFORMATION

Corresponding Author

Nitash P. Balsara − *Department of Chemical and Biomolecular Engineering, University of California−Berkeley, Berkeley, California 94720, United States; Materials Sciences Division and Joint Center for Energy Storage Research (JCESR), Lawrence Berkeley National Lab, Berkeley, California 94720, United States;* orcid.org/0000-0002-0106-5565; Email: nbalsara@berkeley.edu

Authors

Whitney S. Loo − *Department of Chemical and Biomolecular Engineering, University of California−Berkeley, Berkeley, California 94720, United States;* orcid.org/0000-0002-9773-3571

Antonio Faraone − *National Institute of Standards and Technology Center for Neutron Research, Gaithersburg, Maryland 20899, United States*

Lorena S. Grundy − *Department of Chemical and Biomolecular Engineering, University of California−Berkeley, Berkeley, California 94720, United States;* orcid.org/0000-0001-7706-2216

Kevin W. Gao − *Department of Chemical and Biomolecular Engineering, University of California−Berkeley, Berkeley, California 94720, United States;* orcid.org/0000-0002-6794-1265

Complete contact information is available at: https://pubs.acs.org/10.1021/acsmacrolett.0c00236

Author Contributions

The manuscript was written through contributions of all authors. All authors have given approval to the final version of the manuscript.

Notes

The authors declare no competing financial interest.

■ ACKNOWLEDGMENTS

This work was intellectually led by the Joint Center for Energy Storage Research (JCESR), an Energy Innovation Hub funded by the U.S. Department of Energy (DOE), Office of Science, Basic Energy sciences (BES), under Contract No. DEAC02-06CH11357. We acknowledge the support of the National Institute of Standards and Technology, U.S. Department of Commerce, in providing the neutron research facilities used in this work. Access to NGB-30m as well as the NGA-NSE was provided by the Center for High Resolution Neutron Scattering, a partnership between the National Institute of Standards and Technology and the National Science

Foundation under Agreement No. DMR-1508249. W.S.L. acknowledges funding from the National Science Foundation Graduate Student Research Fellowship DGE-1106400. K.W.G. acknowledges funding from a National Defense and Science Engineering Graduate Fellowship. We thank Lutz Wilner and Sangwoo Lee for the guidance on synthesizing isotopically labeled block copolymers. The identification of any commercial product or trade name does not imply endorsement or recommendation by the National Institute of Standards and Technology.

REFERENCES

(1) Tarascon, J. M.; Armand, M. Issues and Challenges Facing Rechargeable Lithium Batteries. *Nature* **2001**, *414* (6861), 359−367.
(2) Lascaud, S.; Perrier, M.; Vallee, A.; Besner, S.; Prud'homme, J.; Armand, M. Phase Diagrams and Conductivity Behavior of Poly-(Ethy1ene Oxide)-Molten Salt Rubbery Electrolytes. *Macromolecules* **1994**, *27* (25), 7469−7477.
(3) Hayamizu, K.; Sugimoto, K.; Akiba, E.; Aihara, Y.; Bando, T.; Price, W. S. An NMR and Ionic Conductivity Study of Ion Dynamics in Liquid Poly(Ethylene Oxide)-Based Electrolytes Doped with LiN(SO2CF3)2. *J. Phys. Chem. B* **2002**, *106* (3), 547−554.
(4) Newman, J.; Thomas-Alyea, K. E. *Electrochemical Systems*; John Wiley & Sons: Hoboken, NJ, 2004.
(5) Teran, A. a.; Tang, M. H.; Mullin, S. a.; Balsara, N. P. Effect of Molecular Weight on Conductivity of Polymer Electrolytes. *Solid State Ionics* **2011**, *203* (1), 18−21.
(6) Galluzzo, M. D.; Maslyn, J. A.; Shah, D. B.; Balsara, N. P. Ohm's Law for Ion Conduction in Lithium and beyond-Lithium Battery Electrolytes. *J. Chem. Phys.* **2019**, *151* (2), 020901.
(7) Timachova, K.; Watanabe, H.; Balsara, N. P. Effect of Molecular Weight and Salt Concentration on Ion Transport and the Transference Number in Polymer Electrolytes. *Macromolecules* **2015**, *48* (21), 7882−7888.
(8) Becher, M.; Becker, S.; Hecht, L.; Vogel, M. From Local to Diffusive Dynamics in Polymer Electrolytes: NMR Studies on Coupling of Polymer and Ion Dynamics across Length and Time Scales. *Macromolecules* **2019**, *52* (23), 9128−9139.
(9) Devaux, D.; Bouchet, R.; Glé, D.; Denoyel, R. Mechanism of Ion Transport in PEO/LiTFSI Complexes: Effect of Temperature, Molecular Weight and End Groups. *Solid State Ionics* **2012**, *227*, 119−127.
(10) Shi, J.; Vincent, C. A. The Effect of Molecular Weight on Cation Mobility in Polymer Electrolytes. *Solid State Ionics* **1993**, *60* (1−3), 11−17.
(11) Mao, G.; Perea, R. F.; Howells, W. S.; Price, D. L.; Saboungi, M.-L. Relaxation in Polymer Electrolytes on the Nanosecond Timescale. *Nature* **2000**, *405*, 163−165.
(12) Mao, G.; Saboungi, M. L.; Price, D. L.; Armand, M.; Mezei, F.; Pouget, S. α-Relaxation in PEO-LiTFSI Polymer Electrolytes. *Macromolecules* **2002**, *35* (2), 415−419.
(13) Mongcopa, K. I. S.; Gribble, D. A.; Loo, W. S.; Tyagi, M.; Mullin, S. A.; Balsara, N. P. Segmental Dynamics Measured by Quasi-Elastic Neutron Scattering and Ion Transport in Chemically Distinct Polymer Electrolytes. *Macromolecules* **2020**, na DOI: 10.1021/acs.macromol.0c00091.
(14) Fullerton-Shirey, S. K.; Maranas, J. K. Effect of LiClO 4 on the Structure and Mobility of PEO-Based Solid Polymer Electrolytes. *Macromolecules* **2009**, *42* (6), 2142−2156.
(15) Mongcopa, K. I. S.; Tyagi, M.; Mailoa, J. P.; Samsonidze, G.; Kozinsky, B.; Mullin, S. A.; Gribble, D. A.; Watanabe, H.; Balsara, N. P. Relationship between Segmental Dynamics Measured by Quasi-Elastic Neutron Scattering and Conductivity in Polymer Electrolytes. *ACS Macro Lett.* **2018**, *7* (4), 504−508.
(16) Webb, M. A.; Yamamoto, U.; Savoie, B. M.; Wang, Z. G.; Miller, T. F. Globally Suppressed Dynamics in Ion-Doped Polymers. *ACS Macro Lett.* **2018**, *7* (6), 734−738.
(17) Frischknecht, A. L.; Paren, B. A.; Middleton, L. R.; Koski, J. P.; Tarver, J. D.; Tyagi, M.; Soles, C. L.; Winey, K. I. Chain and Ion Dynamics in Precise Polyethylene Ionomers. *Macromolecules* **2019**, *52* (20), 7939−7950.
(18) Do, C.; Lunkenheimer, P.; Diddens, D.; Götz, M.; Weiß, M.; Loidl, A.; Sun, X. G.; Allgaier, J.; Ohl, M. Li+ Transport in Poly(Ethylene Oxide) Based Electrolytes: Neutron Scattering, Dielectric Spectroscopy, and Molecular Dynamics Simulations. *Phys. Rev. Lett.* **2013**, *111* (1), 1−5.
(19) Bresser, D.; Lyonnard, S.; Iojoiu, C.; Picard, L.; Passerini, S. Decoupling Segmental Relaxation and Ionic Conductivity for Lithium-Ion Polymer Electrolytes. *Mol. Syst. Des. Eng.* **2019**, *4* (4), 779−792.
(20) Choo, Y.; Halat, D. M.; Villaluenga, I.; Timachova, K.; Balsara, N. P. Diffusion and Migration in Polymer Electrolytes. *Prog. Polym. Sci.* **2020**, *103*, 101220.
(21) Seo, Y.; Shen, K. H.; Brown, J. R.; Hall, L. M. Role of Solvation on Diffusion of Ions in Diblock Copolymers: Understanding the Molecular Weight Effect through Modeling. *J. Am. Chem. Soc.* **2019**, *141*, 18455.
(22) Monroe, C.; Newman, J. Dendrite Growth in Lithium/Polymer Systems. *J. Electrochem. Soc.* **2003**, *150* (10), A1377.
(23) Gallagher, K. G.; Goebel, S.; Greszler, T.; Mathias, M.; Oelerich, W.; Eroglu, D.; Srinivasan, V. Quantifying the Promise of Lithium-Air Batteries for Electric Vehicles. *Energy Environ. Sci.* **2014**, *7* (5), 1555−1563.
(24) Lin, D.; Liu, Y.; Cui, Y. Reviving the Lithium Metal Anode for High-Energy Batteries. *Nat. Nanotechnol.* **2017**, *12* (3), 194−206.
(25) Hasan, N.; Pulst, M.; Samiullah, M. H.; Kressler, J. Comparison of Li+-Ion Conductivity in Linear and Crosslinked Poly(Ethylene Oxide). *J. Polym. Sci., Part B: Polym. Phys.* **2019**, *57* (1), 21−28.
(26) Soo, P. P.; Huang, B.; Jang, Y.-I.; Chiang, Y.-M.; Sadoway, D. R.; Mayes, A. M. Rubbery Block Copolymer Electrolytes for Solid-State Rechargeable Lithium Batteries. *J. Electrochem. Soc.* **1999**, *146* (1), 32−37.
(27) Panday, A.; Mullin, S.; Gomez, E. D.; Wanakule, N.; Chen, V. L.; Hexemer, A.; Pople, J.; Balsara, N. P. Effect of Molecular Weight and Salt Concentration on Conductivity of Block Copolymer Electrolytes. *Macromolecules* **2009**, *42* (13), 4632−4637.
(28) Young, W. S.; Kuan, W. F.; Epps, T. H. Block Copolymer Electrolytes for Rechargeable Lithium Batteries. *J. Polym. Sci., Part B: Polym. Phys.* **2014**, *52* (1), 1−16.
(29) Galluzzo, M. D.; Loo, W. S.; Wang, A. A.; Walton, A.; Maslyn, J. A.; Balsara, N. P. Measurement of Three Transport Coefficients and the Thermodynamic Factor in Block Copolymer Electrolytes with Different Morphologies. *J. Phys. Chem. B* **2020**, *124* (5), 921−935.
(30) Rouse, P. E. A Theory of the Linear Viscoelastic Properties of Dilute Solutions of Coiling Polymers. *J. Chem. Phys.* **1953**, *21* (7), 1272−1280.
(31) Doi, M.; Edwards, S. F. *The Theory of Polymer Dynamics*; Oxford University Press: Oxford, U.K., 1986.
(32) De Gennes, P. G. Reptation of a Polymer Chain in the Presence of Fixed Obstacles. *J. Chem. Phys.* **1971**, *55* (2), 572−579.
(33) Montes, H.; Monkenbusch, M.; Willner, L.; Rathgeber, S.; Fetters, L.; Richter, D. Neutron Spin Echo Investigation of the Concentration Fluctuation Dynamics in Melts of Diblock Copolymers. *J. Chem. Phys.* **1999**, *110* (20), 10188−10202.
(34) Oparaji, O.; Narayanan, S.; Sandy, A.; Ramakrishnan, S.; Hallinan, D. Structural Dynamics of Strongly Segregated Block Copolymer Electrolytes. *Macromolecules* **2018**, *51* (7), 2591−2603.
(35) Hadjichristidis, N.; Pitsikalis, M.; Pispas, S.; Iatrou, H. Polymers with Complex Architecture by Living Anionic Polymerization. *Chem. Rev.* **2001**, *101* (12), 3747−3792.
(36) Hadjichristidis, N.; Iatrou, H.; Pispas, S.; Pitsikalis, M. Anionic Polymerization: High Vacuum Techniques. *J. Polym. Sci., Part A: Polym. Chem.* **2000**, *38* (18), 3211−3234.
(37) Quirk, R. P.; Kim, J.; Kausch, C.; Chun, M. Butyllithium-Initiated Anionic Synthesis of Well-Defined Poly(Styrene-Block-

https://dx.doi.org/10.1021/acsmacrolett.0c00236
ACS Macro Lett. 2020, 9, 639−645

Ethylene Oxide) Block Copolymers with Potassium Salt Additives. *Polym. Int.* **1996**, *39* (1), 3−10.
(38) Loo, W. S.; Sethi, G. K.; Teran, A. A.; Galluzzo, M. D.; Maslyn, J. A.; Oh, H. J.; Mongcopa, K. I.; Balsara, N. P. Composition Dependence of the Flory−Huggins Interaction Parameters of Block Copolymer Electrolytes and the Isotaksis Point. *Macromolecules* **2019**, *52* (15), 5590−5601.
(39) Richter, B. D.; Ewen, B. Neutron Spin-Echo Investigations on the Dynamics of Polymers. *J. Appl. Crystallogr.* **1988**, *21*, 715−728.
(40) Loo, W. S.; Mongcopa, K. I.; Gribble, D. A.; Faraone, A. A.; Balsara, N. P. Investigating the Effect of Added Salt on the Chain Dimensions of Poly(Ethylene Oxide) through Small-Angle Neutron Scattering. *Macromolecules* **2019**, *52*, 8724−8732.
(41) Glinka, C. J.; Barker, J. G.; Hammouda, B.; Krueger, S.; Moyer, J. J.; Orts, W. J. The 30 m Small-Angle Neutron Scattering Instruments at the National Institute of Standards and Technology. *J. Appl. Crystallogr.* **1998**, *31* (3), 430−445.
(42) Kline, S. *SANS Data Reduction Tutorial*; NIST Center for Neutron Research, 2001.
(43) Kline, S. R. Reduction and Analysis of SANS and USANS Data Using IGOR Pro. *J. Appl. Crystallogr.* **2006**, *39* (6), 895−900.
(44) Azuah, R. T.; Kneller, L. R.; Qiu, Y.; Tregenna-Piggott, P. L. W.; Brown, C. M.; Copley, J. R. D.; Dimeo, R. M. DAVE: A Comprehensive Software Suite for the Reduction, Visualization, and Analysis of Low Energy Neutron Spectroscopic Data. *J. Res. Natl. Inst. Stand. Technol.* **2009**, *114* (6), 341.
(45) Loo, W. S.; Galluzzo, M. D.; Li, X.; Maslyn, J. A.; Oh, H. J.; Mongcopa, K. I.; Zhu, C.; Wang, A. A.; Wang, X.; Garetz, B. A.; Balsara, N. P. Phase Behavior of Mixtures of Block Copolymers and a Lithium Salt. *J. Phys. Chem. B* **2018**, *122* (33), 8065−8074.
(46) Wanakule, N. S.; Virgili, J. M.; Teran, A. A.; Wang, Z. G.; Balsara, N. P. Thermodynamic Properties of Block Copolymer Electrolytes Containing Imidazolium and Lithium Salts. *Macromolecules* **2010**, *43* (19), 8282−8289.
(47) Teran, A. a.; Balsara, N. P. Thermodynamics of Block Copolymers with and without Salt. *J. Phys. Chem. B* **2014**, *118* (1), 4−17.
(48) Nakamura, I.; Wang, Z.-G. Salt-Doped Block Copolymers: Ion Distribution, Domain Spacing and Effective χ Parameter. *Soft Matter* **2012**, *8* (36), 9356.
(49) Loo, W. S.; Balsara, N. P. Organizing Thermodynamic Data Obtained from Multicomponent Polymer Electrolytes: Salt-containing Polymer Blends and Block Copolymers. *J. Polym. Sci., Part B: Polym. Phys.* **2019**, *57* (18), 1177−1187.
(50) de Gennes, P. G. *Scaling Concepts in Polymer Chemsitry*; Cornell University Press: Ithaca, NY, 1979.
(51) Richter, D.; Monkenbusch, M.; Arbe, A.; Colmenero, J. Neutron Spin Echo in Polymer Systems. *Adv. Polym. Sci.* **2005**, *174*, 1−221.
(52) De Gennes, P. G. Coherent Scattering by One Reptating Chain. *J. Phys. (Paris)* **1981**, *42* (5), 735−740.
(53) Niedzwiedz, K.; Wischnewski, A.; Pyckhout-Hintzen, W.; Allgaier, J.; Richter, D.; Faraone, A. Chain Dynamics and Viscoelastic Properties of Poly(Ethylene Oxide). *Macromolecules* **2008**, *41* (13), 4866−4872.
(54) Senses, E.; Ansar, S. M.; Kitchens, C. L.; Mao, Y.; Narayanan, S.; Natarajan, B.; Faraone, A. Small Particle Driven Chain Disentanglements in Polymer Nanocomposites. *Phys. Rev. Lett.* **2017**, *118* (14), 147801.
(55) Richter, D.; Farago, B.; Butera, R.; Fetters, L. J.; Huang, J. S.; Ewen, B. On the Origins of Entanglement Constraints. *Macromolecules* **1993**, *26* (4), 795−804.
(56) Fetters, L. J.; Lohse, D. J.; Richter, D.; Witten, T. A.; Zirkel, A. Connection between Polymer Molecular Weight, Density, Chain Dimensions, and Melt Viscoelastic Properties. *Macromolecules* **1994**, *27*, 4639−4647.
(57) Wittmer, J.; Paul, W.; Binder, K. Rouse and Reptation Dynamics at Finite Temperatures: A Monte Carlo Simulation. *Macromolecules* **1992**, *25* (26), 7211−7219.
(58) Dalvi, M. C.; Eastman, C. E.; Lodge, T. P. Diffusion in Microstructured Block Copolymers: Chain Localization and Entanglements. *Phys. Rev. Lett.* **1993**, *71* (16), 2591−2594.
(59) Lodge, T. P.; Dalvi, M. C. Mechanisms of Chain Diffusion in Lamellar Block Copolymers. *Phys. Rev. Lett.* **1995**, *75* (4), 657−660.
(60) Lodge, T. P.; Hamersky, M. W.; Milhaupt, J. M.; Kannan, R. M.; Dalvi, M. C.; Eastman, C. E. Diffusion in Microstructured Block Copolymer Melts. *Macromol. Symp.* **1997**, *121* (1), 219−233.
(61) Senses, E.; Tyagi, M.; Pasco, M.; Faraone, A. Dynamics of Architecturally Engineered All-Polymer Nanocomposites. *ACS Nano* **2018**, *12* (11), 10807−10816.
(62) Molinari, N.; Mailoa, J. P.; Kozinsky, B. Effect of Salt Concentration on Ion Clustering and Transport in Polymer Solid Electrolytes: A Molecular Dynamics Study of PEO-LiTFSI. *Chem. Mater.* **2018**, *30* (18), 6298−6306.
(63) Brooks, D. J.; Merinov, B. V.; Goddard, W. A.; Kozinsky, B.; Mailoa, J. Atomistic Description of Ionic Diffusion in PEO-LiTFSI: Effect of Temperature, Molecular Weight, and Ionic Concentration. *Macromolecules* **2018**, *51* (21), 8987−8995.
(64) Borodin, O.; Smith, G. D. Molecular Dynamics Simulations of Poly(Ethylene Oxide)/LiI Melts. 1. Structural and Conformational Properties. *Macromolecules* **1998**, *31* (23), 8396−8406.
(65) Rubinstein, M.; Colby, R. H. *Polymer Physics*; Oxford University Press: Oxford, U.K., 2003.
(66) Gribble, D. A.; Frenck, L.; Shah, D. B.; Maslyn, J. A.; Loo, W. S.; Mongcopa, K. I. S.; Pesko, D. M.; Balsara, N. P. Comparing Experimental Measurements of Limiting Current in Polymer Electrolytes with Theoretical Predictions. *J. Electrochem. Soc.* **2019**, *166* (14), A3228−A3234.
(67) Pesko, D. M.; Feng, Z.; Sawhney, S.; Newman, J.; Srinivasan, V.; Balsara, N. P. Comparing Cycling Characteristics of Symmetric Lithium-Polymer-Lithium Cells with Theoretical Predictions. *J. Electrochem. Soc.* **2018**, *165* (13), A3186−A3194.

https://dx.doi.org/10.1021/acsmacrolett.0c00236
ACS Macro Lett. 2020, 9, 639−645